

**Development and Evaluation of a Model of Lidocaine's Action
on Cardiac Sodium Channels**

Lisa A. Irvine, M. Saleet Jafri, and Raimond L. Winslow

Department of Biomedical Engineering and
Center for Computational Medicine & Biology
The Johns Hopkins University School of Medicine
Baltimore, MD 21205

Running title: Model of Lidocaine's Action

Keywords: modal gating; hH1 channel; antiarrhythmic drugs; modulated receptor hypothesis

Correspondence to:

Raimond L. Winslow
The Johns Hopkins University School of Medicine
Department of Biomedical Engineering
411 Traylor Building, 720 Rutland Avenue
Baltimore, MD 21205
Phone: (410) 502-5090
Fax: (410) 614-0166
E-mail: rwinslow@bme.jhu.edu

ABSTRACT

Several models have been proposed to explain the block of cardiac sodium channels by lidocaine; however, none has been successful in reproducing a wide range of drug effects. In this study, a new model of lidocaine's action is formulated based on the modulated receptor hypothesis and a Markov model of the cardiac sodium channel. In the presence of lidocaine, the model consists of a population of drug bound channels and a population of non-drug bound channels. Channels in the drug bound population are assumed to have modified gating kinetics in accordance with experimental data and to satisfy microscopic reversibility. The lidocaine concentration and rates of drug binding and unbinding determine the relative size of each population and the observed effect of the drug. This model reproduces a wide range of drug effects including use-dependence, onset of block, recovery from block, the dose-response curve, the steady-state inactivation curve, and the charge-voltage curve and has reasonable drug affinities for each state. Thus, the model significantly improves on previous models of lidocaine's action.

INTRODUCTION

The modulated receptor (MR) hypothesis states that the affinity of a receptor for drug changes as the channel changes state (Hille, 1977; Hondeghem and Katzung, 1977). In order to preserve energy balances while permitting state-dependent binding, this hypothesis requires gating of drug bound channels to be modified. Recent experiments show that for lidocaine, gating of drug bound channels is indeed altered. QX-222, a quaternary derivative of lidocaine, dramatically reduces the slope and maximum charge of the charge-voltage relationship (Hanck, et al., 1994). Lidocaine also prevents bursting, thus decreasing the probability of occupying the slow-inactivating mode. As evidenced by an increase in null sweeps, lidocaine also increases the probability of occupying a “non-conducting mode” (Nilius, et al., 1987). Finally, lidocaine not only slows the rate of recovery from inactivation, but also prolongs the initial delay associated with deactivation before recovery occurs (Nuss, et al., 1995).

A quantitative model of lidocaine’s action based on the MR hypothesis (Hondeghem and Katzung, 1977) has been formulated and analyzed (Irvine, et al., submitted to *Biophys. J.*). This model reproduces a range of drug actions including use-dependence, rate of block onset, rate of recovery from block, and the dose-response curve (Irvine, et al., submitted to *Biophys. J.*). However, the model parameters that reproduce these data do not yield reasonable drug affinities for each state, do not preserve microscopic reversibility, and do not reproduce changes in the charge-voltage relationship which have been measured experimentally. This model fails for two reasons: a) it is based on an inaccurate description of the underlying cardiac sodium channel; and b) it does not adequately describe the mechanism of drug action.

In this study, a new MR model of lidocaine's action is formulated using a recently developed Markov state model of the cardiac sodium channel (Irvine et al, 1999). In the presence of lidocaine, the model consists of a population of drug bound channels and a population of non-drug bound channels. The lidocaine concentration and rates of drug binding and unbinding determine the relative size of each population and the observed effect of the drug. Using these different populations of channels, a wide range of drug effects is reproduced and new understanding of the mechanism of lidocaine's action is gained.

METHODS

Model

Figure 1 shows the gating schemes of the non-drug bound (A) and drug bound (B) populations and the transitions between these two populations (C). The gating scheme of the non-drug bound channels is the model of the cardiac sodium channel published previously (Irvine, et al., 1999). The top row of states corresponds to zero to four voltage sensors being activated (C_0 through C_4) plus an additional conformational change required for opening ($C_4 \rightarrow O_1$ and $C_4 \rightarrow O_2$). The bottom row of states corresponds to the inactivation particle blocking the pore at each position of the voltage sensors. All transitions are voltage dependent except for those between closed and closed-inactivated states, which are voltage independent. Rate constants are from Eyring rate theory (Hille, 1992)

$$k_{ij} = \frac{kT}{h} \exp\left[-\frac{H_{ij}^\ddagger}{RT}\right] \exp\left[-\frac{z_{ij}FV}{RT}\right] \quad (1)$$

where k is the Boltzmann constant, T is the absolute temperature, h is the Planck constant, R is the gas constant, F is Faraday's constant, ΔH is the change in enthalpy, ΔS is the change in entropy, z is the effective valence (ie., the charge moved times the fractional distance the charge is moved through the membrane), and V is membrane potential in volts. The model's rate constants are formulated so that microscopic reversibility is preserved.

Transitions between drug bound and non-drug bound populations are permitted only between the open states, the closed-inactivated states, and the inactivated state (Fig. 1C). The affinities of the closed states for drug are low. Thus, transitions between populations rarely occur from these states and drug bound channels are rarely closed. Therefore, transitions between populations from the closed states and closed-drug bound states are excluded from the model.

To minimize the number of free parameters, the rates of drug binding and unbinding to the closed-inactivated states are assumed to increase by a scaling factor (g) with transition towards the inactivated state. Similarly, the rates of drug unbinding from the closed-inactivated states are decreased by a scaling factor (h) with transition towards the inactivated state. As a result of scaling the binding and unbinding rates, the drug affinities of the closed-inactivated states increase with transition towards the inactivated state.

To satisfy microscopic reversibility around the closed-inactivated-closed-inactivated-drug bound loop, the gating kinetics of the drug bound channels must be altered. Microscopic reversibility can be satisfied using two different modifications. Figure 1B shows the modifications that yield the better prediction of the charge-voltage

curve. Using these modifications, forward rate constants are multiplied by the scaling factor h , while reverse rate constants are divided by the scaling factor g . Microscopic reversibility must also be satisfied around the open-inactivated-drug bound loop. The rate of inactivating from the “open”-drug bound state (D_1) is assumed to be a constant f times the rate of inactivation in the normal mode (O_n). The rate of reopening from the inactivated drug bound state is then

$$O_f^* = \frac{k_A l_I f O_f}{k_I l_A} \quad (2)$$

where k_A and l_A are the drug binding and unbinding rates, respectively, for the open states, k_I and l_I are the drug binding and unbinding rates, respectively, for the inactivated state, O_f is the rate of reopening from the inactivated state in the normal mode, and f is as defined above.

Determination of the Model Parameters

Parameters of the model are determined by fitting a variety of experimental data sets describing lidocaine’s action. The probability of occupying any particular channel state is described mathematically by a set of ordinary differential equations, written in matrix notation as

$$\frac{d\mathbf{P}(t)}{dt} = \mathbf{W}\mathbf{P}(t), \quad (3)$$

where $\mathbf{P}(t)$ is a vector describing the probabilities of occupying each state and \mathbf{W} is the transition matrix. In general, \mathbf{W} will be a function of voltage and thus time. For voltage-clamped conditions, however, \mathbf{W} is time-independent; thus Eq. 3 has the analytic solution

$$\mathbf{P}(t) = \exp(\mathbf{W}t)\mathbf{P}(0). \quad (4)$$

Equation 4 is solved on a Silicon Graphics computer using linear algebra subroutines from the Silicon Graphics mathematics library (complib.sgimath).

Five different data sets at a lidocaine concentration of 200 μ M (Furukawa, et al., 1995) and a dose-response curve (Jia, et al., 1993) are used to determine the model parameters. The first data set describes use-dependence. Use-dependent block is induced by applying a train of 3 ms depolarizing pulses from -140 mV to -20 mV at a rate of 5 Hz (Furukawa, et al., 1995). The second and third data sets describe the rate of block onset due to a -80 mV and a -20 mV conditioning pulse of varying duration. The extent of block is measured using a 30 ms test pulse to -20 mV after a 500 ms recovery interval at -140 mV (Furukawa, et al., 1995). The fourth data set describes the rate of recovery from block. Block is induced by applying a train of 10 ms depolarizing pulses from -140 mV to -20 mV at a rate of 30 Hz. The extent of recovery is then measured using a 30 ms test pulse to -20 mV after holding at -140 mV for various intervals (Furukawa, et al., 1995). The fifth data set describes the steady-state availability curve in the presence of lidocaine. A 500 ms conditioning prepulse to a potential between -150 mV and -20 mV is applied. The current is then measured at 0 mV. Finally, the dose-response curve used here is defined as the fraction of unblocked sodium current elicited by the twentieth pulse of a 2 Hz train versus the drug concentration. Pulses are from -140 mV to -20 mV for 10 ms (Jia, et al., 1993). Together these data sets reflect drug binding (onset data), drug unbinding (recovery data), the balance between binding and unbinding (use-dependence data), and concentration-dependence (dose-response data).

The drug binding (k_A, k_I) and unbinding rates (l_R, l_A, l_I) and the scaling factors f, g , and h are parameters to be determined by fitting model responses to experimental data.

The rate of drug binding to the closed-inactivated states (k_R) is determined by satisfying microscopic reversibility around the closed-inactivated-inactivated-drug bound loop according to the following equation:

$$k_R = \frac{k_I l_R}{l_I g^5 h^5}. \quad (5)$$

Parameters are determined using a simulated annealing algorithm (Corana, et al., 1987). This algorithm minimizes the cost function, which is the weighted sum of the least-squared errors between model responses and experimental data, by randomly searching the parameter space and incrementally decreasing the search radius. Whereas many minimization algorithms accept only downhill moves and tend to converge on local minima, the simulated annealing algorithm accepts uphill moves as well and thus, is more likely to find the global minimum. Uphill moves are accepted based on the Metropolis criterion, a probabilistic function determined from the difference between new and old errors and the annealing temperature. The annealing temperature controls the rate of convergence by influencing what uphill moves are accepted and by limiting the search radius. In order to reach a minimum, as the algorithm converges on a solution, the annealing temperature is decreased by 5% per 50N function evaluations, where N is the number of parameters to be determined.

RESULTS

Several sets of parameters were found that yielded good fits of model responses to experimental data. The parameters that gave affinities closest to the experimental affinities were chosen and are listed in Table 1. The resulting affinity of the inactivated state for lidocaine is 11 μ M. The inactivated state affinity is within the range of

experimental values (10 to 27 μM) (Bean, et al., 1983; Furukawa, et al., 1995; Nuss, et al., 1995). Affinities of the closed-inactivated states for lidocaine range from 628 μM for C_0I to 24 μM for C_4I . The model closed-inactivated state (C_0I) has an affinity similar to that of the resting state in the literature (402 to 669 μM) (Bean, et al., 1983; Furukawa, et al., 1995; Nuss, et al., 1995). The model's open state affinity is 23 μM . This affinity is difficult to compare with experimental values. Bennett disabled inactivation by mutating three amino acids in the III-IV interdomain to glutamines and calculated the open state affinity to be 600 μM (Bennett, et al., 1995). However, it is unclear whether the open state affinity is unchanged if inactivation is disabled. Another study estimates the open state affinity to be 47 μM , which is similar to the model's value (Furukawa, et al., 1995). Although the exact affinity of the open state is difficult to measure, experimental studies agree that it is less than that of the inactivated state (Bean, et al., 1983; Kodama, et al., 1990; Bennett, et al., 1995), as is the case in this model.

The model is able to reproduce a wide range of experimental data. Figure 2 shows the model's fit to three of the data sets used to determine the model parameters. The model reproduces use-dependence (Fig. 2A), the rate of recovery from block at -140 mV (Fig. 2B), and the dose-response curve (Fig. 2C) well. The use-dependence and recovery curves are fit using a single exponential. For the use-dependence data, the time constants are 2.5 and 3 pulses for the experimental data and the model, respectively. For the recovery data, the time constants are 793 ms and 794 ms, respectively. The dose-response curves are fit using a sigmoidal curve of the form:

$$\frac{I}{I_{\text{nodrug}}} = \frac{1}{1 + \frac{[\text{lidocaine}]}{IC_{50}}} \quad (6)$$

where the IC_{50} is the drug concentration at which the current is reduced by 50%. The IC_{50} values are 166 μ M and 193 μ M for the experimental data and the model, respectively.

Figure 3 shows the model's fit to the data sets describing the rate of block onset, which were also used to determine the model parameters. The rate of block development at both potentials is reproduced by the model. For -20 mV (Fig. 3A), the data is best fit using the sum of two exponentials. The time constants are 5.7 ms and 181 ms for the experimental data and 6.2 ms and 964 ms for the model, respectively. The fast time constants are similar, but the model's slow time constant is much too large. This time constant can be decreased by making the affinity of the open state greater than that of the inactivated state. However, such a change results in affinities that contradict the experimental data (Bean, et al., 1983; Kodama, et al., 1990; Bennett, et al., 1995). For -80 mV (Fig. 3B), the data is fit using a single exponential. The time constants are 360 ms and 357 ms for the experimental data and the model, respectively.

The final data set used to determine the model parameters is steady-state availability. Figure 4A shows the steady-state availability curves in the absence of drug and in the presence of 200 μ M lidocaine. Both curves are fit using a Boltzmann function. The slope factor and half-maximal potential values are -12.5 mV and -104.2 mV for the experimental data and -13 mV and -120 mV for the model, respectively. The 200 μ M lidocaine concentration produces a 15.8 mV hyperpolarizing shift of the steady-state inactivation curve without any significant change in the slope factor. This shift is similar to that measured experimentally (11 mV in the hyperpolarizing direction) (Furukawa, et al., 1995). Figure 4B shows the steady-state availability curve in the presence of 25 μ M

lidocaine. A Boltzmann fit to this curve yields slope factor and half-maximal potential values of -13.1 mV and -111.5 mV. The $25 \mu\text{M}$ lidocaine concentration produces a much smaller shift of 7.2 mV. Thus, the model predicts that the shift in the steady-state availability curve is a function of drug concentration. This prediction is supported by experimental data which shows that the shift of the steady-state availability curve increases as the lidocaine concentration is increased (Bean, et al., 1983).

In addition to being able to reproduce data used to determine the model parameters, the model can predict experimental data sets not used in the fitting procedure. Figure 5 shows the model's ability to predict the rate of block development for use-dependent protocols of different frequencies and pulse durations of 3 ms (Fig. 5A) and 10 ms (Fig. 5B). As the interstimulus interval (ISI) is decreased, it takes more pulses to reach steady-state and more block is produced. For any ISI, a longer pulse duration results in more block. These results can be compared to those of Furukawa and coworkers (Fig. 6b in Furukawa, et al., 1995). The number of pulses needed to reach steady-state and the steady-state block for different ISIs are very similar in the model and the experimental data. However, there are minor differences between model responses and experimental data at particular ISIs and pulse durations. At low frequencies, the rate at which the model approaches steady-state is somewhat slower than indicated by the experimental data. The model also predicts too little block at high frequencies for 10 ms pulse durations. Despite these differences, the model is able to predict features of the use-dependence data over a broad range of frequencies and pulse durations.

Another data set predicted by the model is the reduction in sodium current due to lidocaine. Figure 6A compares current tracings for a clamp voltage of -30 mV in the

absence of lidocaine and in the presence of 25 μ M and 200 μ M lidocaine. Lidocaine reduces the peak current without changing the kinetics of activation or inactivation. At this clamp potential, 25 μ M lidocaine reduces the peak current by 5.9%; 200 μ M lidocaine reduces the peak current by 34.8%. Furukawa and coworkers found that 200 μ M lidocaine reduced the peak current by $24.5 \pm 2.9\%$ (Furukawa, et al., 1995). Thus, the model predicts slightly more reduction in peak current at -30 mV than the experimental data shows. Figure 6B shows the current-voltage curves in the absence of lidocaine and in the presence of 25 μ M and 200 μ M lidocaine. Lidocaine reduces the magnitude of the current at each potential without altering the shape of the curve. Each curve is fit using a modified Boltzmann function. In the absence of lidocaine, the conductance (G_{Na}), slope factor (s), and half-maximal potential ($V_{0.5}$) values are 0.0154 mV^{-1} , 7.0 mV, and -47.1 mV, respectively. For 25 μ M lidocaine, there is little change in these values; G_{Na} is 0.0147 mV^{-1} , s is 7.1 mV, and $V_{0.5}$ is -46.6 mV. For 200 μ M lidocaine, G_{Na} is 0.0109 mV^{-1} , s is 7.6 mV, and $V_{0.5}$ is -44.2 mV. Thus, for 200 μ M lidocaine, the model predicts a 29.2% reduction in conductance, a 0.6 mV increase in slope factor, and a 2.9 mV rightward shift in the half-maximal potential. The experimental data shows a $22.6 \pm 1.7\%$ decrease in conductance for 200 μ M lidocaine (Furukawa, et al., 1995). The model prediction is therefore in approximate agreement with the experimental data. The change in slope factor and half-maximal potential are small and are close to the range of variation observed experimentally. The model therefore agrees with the experimental data in predicting no significant change in the slope factor or half-maximal potential (Furukawa, et al., 1995).

The model also predicts the experimentally observed changes in the charge-voltage curve due to lidocaine. Block is developed by applying a 130 pulse train from -150 mV to 0 mV at 10 Hz. After a 90 ms interval at -150 mV, a test pulse is applied and the gating charge is computed. Figure 7A compares the charge-voltage curves in the absence of drug and in the presence of 200 μ M lidocaine. A Boltzmann function is fit to each curve. In the absence of drug, the maximum charge is normalized to one and the slope factor and half-maximal potential values are 19 mV and -75 mV, respectively. In the presence of drug, the maximum charge moved is a fraction of the charge moved in the absence of drug and is a parameter to be determined when fitting the Boltzmann function. For 200 μ M lidocaine, the maximum charge is 0.587 and the slope factor and half-maximal potential values are 22.3 mV and -92.1 mV, respectively. Therefore, lidocaine reduces the amount of charge moved by 41.3% , reduces the slope of the charge-voltage curve, and shifts the half-maximal potential 17.1 mV leftward. Experimental data suggest that the lidocaine concentration at which the maximum charge is reduced by 50% is 200 μ M (Hanck, et al., 1992). In addition, although no data exist on the change in the slope factor and half-maximal potential of the charge-voltage curve for 200 μ M lidocaine, studies using 1 mM QX-222, a quaternary derivative of lidocaine, show almost a twofold reduction in slope factor and a leftward shift of the half-maximal potential of 27 mV (Hanck, et al., 1994). Therefore, the model's predictions of lidocaine's effect on the charge-voltage curve are similar to experimental data in the literature. Furthermore, experimental data suggest that the change in the charge-voltage curve is concentration-dependent (Hanck, et al., 1994; Josephson and Cui, 1994). Figure 7B shows the charge-voltage curve for 25 μ M lidocaine. The maximum charge, slope factor, and half-

maximal potential values from a Boltzmann fit are 0.840, 21.8 mV, and -78.5 mV, respectively. Thus, at this lidocaine concentration, there is only a 26% reduction in charge and a leftward shift of the half-maximal potential of 3.5 mV. The model's prediction of a 26% reduction in charge for 25 μ M lidocaine is similar to the experimental data, which show a 24% reduction in charge for 20 μ M lidocaine (Josephson and Cui, 1994). There are no data at this lidocaine concentration on the shift of the half-maximal potential. However, studies done with various concentrations of QX-222 show that the maximum charge is reduced and the slope factor and shift of half-maximal potential are increased as the drug concentration is increased (Hanck, et al., 1994).

Finally, the model can predict how single channel behavior is altered in the presence of lidocaine. Twelve hundred channels are simulated for a 40 ms sweep using a Monte Carlo method described by Clay and DeFelice (Clay and DeFelice, 1983). Open durations and the probability of a null sweep are examined for a voltage range of -70 mV to -10 mV. Figures 8A and 8B show the open duration densities for a clamp voltage of -50 mV in the absence of drug and in the presence of 200 μ M lidocaine. In the absence of drug, most openings are less than 2 ms, although several openings are much longer. In the presence of 200 μ M lidocaine, the openings are shorter and there are almost no long openings. The reduction in long openings due to lidocaine is similar to that seen in single channel experiments (Nilius, et al., 1987). Fitting the open duration densities with a single exponential yields time constants of 0.62 ms and 0.42 ms for the no drug and 200 μ M lidocaine data, respectively. For 200 μ M lidocaine, the open durations are reduced throughout the voltage range tested. The greatest reduction occurs for voltages between

-40 mV and -60 mV, inclusive, where time constants fit to the open duration densities are reduced by approximately 30%. At these potentials, inactivation is relatively slow and channels often close and reopen before they inactivate. The presence of lidocaine provides an additional relatively fast path by which the channel can leave the open state and thus reduces the open duration. At more depolarized potentials, however, channels tend to inactivate quickly. Fewer channels bind lidocaine before inactivating and thus there is less reduction in open durations. For 25 μ M lidocaine, there is very little change in open durations throughout the voltage range tested. Experimental data show that lidocaine does produce a small reduction in open durations, although these studies have been done at low drug concentrations and the concentration-dependence of this reduction is not known (Nilius, et al., 1987; Bennett, et al., 1995). Close inspection of Fig. 8 also shows that the number of openings is reduced in the presence of 200 μ M lidocaine. The probability of a null sweep is increased an average of 10% across the voltage range tested. These results are similar to those of the experimental data, which show that lidocaine increases the number of null sweeps (Nilius, et al., 1987).

DISCUSSION

A new MR model of lidocaine's action on cardiac sodium channels is presented. The model is based on the observation that in the presence of drug, there is a population of drug bound channels and a population of non-drug bound channels. Channels in the drug bound population are assumed to have modified gating kinetics in accordance with experimental data and to satisfy microscopic reversibility. The drug concentration and rates of drug binding and unbinding determine the relative size of each population and the

observed effect of the drug. Rates of drug binding and unbinding are unique for each state of the channel in accordance with the MR hypothesis (Hille, 1977; Hondeghem and Katzung, 1977).

The mechanism of drug action utilized by the model can be described as mode-switching. Experimentally, a single channel is said to exhibit different gating modes when the following criteria are satisfied (Nilius, 1988):

- (1) distinct patterns of channel openings and closings (referred to as gating schemes) coexist within the same recording;
- (2) transitions between these different gating schemes are relatively infrequent;
- (3) chemical or physical agents exist which favor a gating scheme different from the normal scheme.

Although mode-switching has not been proposed previously to explain the effects of sodium channel blockers, it has been used to explain a variety of agent-induced changes in gating kinetics including: a) calcium-mediated inactivation of the calcium current (Imredy and Yue, 1994); b) the action of dihydropyridine calcium agonists and antagonists on L-type calcium channels (Hess, et al., 1984); and c) the effect of luteinizing hormone-releasing hormone on N-type calcium channels (Boland and Bean, 1993).

Several experimental studies show that lidocaine induces changes in gating kinetics. Hanck and colleagues demonstrated that QX-222, a quaternary derivative of lidocaine, dramatically reduces the slope and maximum charge of the charge-voltage relationship (Hanck, et al., 1994). Nilius showed that lidocaine prevents bursting and, as evidenced by an increase in null sweeps, increases the probability of occupying a “non-

conducting mode” (Nilius, et al., 1987). Nuss et al found that lidocaine not only slows the rate of recovery from inactivation, but also prolongs the initial delay associated with deactivation before recovery occurs (Nuss, et al., 1995). Finally, Bennett and coworkers found that for 25 μ M lidocaine, the time constant of drug block is 589 ms – roughly two orders of magnitude larger than that of any process associated with normal gating (Bennett, et al., 1995). These observations demonstrate that lidocaine alters gating kinetics and that the onset of these kinetic changes is relatively slow. Thus, these observations support a mode-switching mechanism of action for lidocaine.

To be classified as a mode-switching model, each mode must exhibit distinctly different gating properties and the rate of transitions between modes must be infrequent relative to the rate of transitions within each mode (Nilius, 1988). The model presented here satisfies these criteria. In general, transitions between normal and drug modes occur at rates much smaller than transition rates within the modes. Specifically, inspection of parameter values in Table 1 shows that transition rates between normal and drug bound closed-inactivated and inactivated states are extremely small. Transitions between modes occur at the fastest rate from the open states. The forward rate k_A of these transitions is dependent on drug concentration. At the highest concentration used in this study (200 μ M), the rate is less than 1 ms^{-1} . Rate constants governing activation and inactivation in the model are in general significantly larger than 1 ms^{-1} (Irvine, et al., 1999). Thus, the model satisfies the criteria of mode-switching, because transitions between modes are relatively infrequent and the drug mode exhibits gating kinetics distinctly different from those of the normal mode.

Both this mode-switching model as well as the Hondeghem-Katzung MR model of lidocaine's action can account quantitatively for use-dependence, rate of block onset, rate of recovery from block, and dose response curves. The model presented here improves on the Hondeghem-Katzung MR model in that it also predicts drug affinities, changes in the charge-voltage curve due to drug, and single channel effects of drug, while preserving microscopic reversibility. The model does so with the addition of only one free parameter beyond that of the Hondeghem-Katzung MR model. Therefore, the predictive capabilities of this new model are not due solely to a large increase in the number of free parameters. Rather, we believe this enhanced predictive power results from two factors: a) the use of a more accurate Markov state model description of the underlying cardiac sodium channel; and b) the simultaneous use of a wide range of experimental data sets to develop and constrain a mechanistically based model of lidocaine's action on this channel.

The advantage of more carefully constraining the model's mechanism of drug action is seen in the model's ability to reproduce the shift in the steady-state inactivation curve and the change in the charge-voltage curve due to lidocaine. Previous models of drug action have reproduced the shift in the steady-state inactivation curve by directly altering the rate of inactivation (Hondeghem and Katzung, 1977; Balser, et al., 1996). For the model presented here, the shift in the steady-state inactivation curve is produced as a result of an increase in the affinities of the closed-inactivated states for lidocaine with transition towards the inactivated state. At very negative potentials, few channels occupy the closed-inactivated states, there is little drug binding, and therefore there is no difference in the steady-state availability curves. As the holding potential is increased,

more channels enter the closed-inactivated states and drug binding occurs. Channels return to the normal mode slowly, so fewer channels are available to conduct than in the absence of drug. With further increases in membrane potential, channels begin to occupy the closed-inactivated states having greater drug affinity and there is an even greater decrease in channel availability.

The reduction in gating charge is also an inherent feature of the model presented here. It is produced simply by excluding certain transitions from the drug bound mode and by altering the rates of transition within the drug mode so as to preserve microscopic reversibility. No changes in the valences are needed to reproduce the changes in the charge-voltage curve. This finding contradicts Hanck's suggestion that gating charge is reduced as a consequence of a reduction in the valence of transitions between drug bound states (Hanck, et al., 1994). Instead, the model suggests that lidocaine interacts with the voltage sensors to slow the channel's entry into certain states and to prevent its entry into other states, thereby altering the charge-voltage curve. Molecular studies to determine how lidocaine interacts with various amino acid residues of the channel are currently being performed. No study has yet determined whether there is an interaction between lidocaine and the voltage sensors. However, it has been shown that lidocaine binds in the pore of the channel (Ragsdale, et al., 1994; Ragsdale, et al., 1996) and, from studies on the *Shaker* potassium channel, that residues in the pore interact with residues in the S4 voltage-sensing segment (Cha and Bezanilla, 1998; Loots and Isacoff, 1998).

There remain some sources of uncertainty in the model's parameters. As noted in RESULTS, several sets of parameters could be found which yielded good fits of the model responses to experimental data. While the affinities of the closed-inactivated and

inactivated states were similar in all sets of parameters, the affinity of the open state varied significantly. Parameters were chosen so that the open state affinity was significantly less than that of the inactivated state in accordance with experimental data (Bean, et al., 1983; Kodama, et al., 1990; Bennett, et al., 1995). However, it is not known by how much the open state affinity differs from that of the inactivated state since there are no good estimates of the open state drug affinity. Estimates range from 47 μ M to 600 μ M depending on the method of calculation (Bennett, et al., 1995; Furukawa, et al., 1995). Better estimates of the open state drug affinity would help to limit the number of possible solutions and would reduce uncertainty in model's parameters.

The model of lidocaine's action presented here has many potential applications. It can be used to study lidocaine's effects on various arrhythmias and diseases such as the long-QT syndrome. In addition, since the mechanism of action of all class I antiarrhythmic drugs is thought to be similar (Hille, 1977; Hondeghem and Katzung, 1977), it may be possible to modify this model in simple ways to account for the action of a broad spectrum of class I antiarrhythmic drugs. Quantitative comparisons of these drugs for the treatment of various arrhythmias could then be performed.

ACKNOWLEDGMENTS

This research was supported by NSF BIR91-17874, NIH HL60133, Silicon Graphics Inc., the Whitaker Foundation, and the Medical Scientist Training Program.

Table 1 – Model parameters

Parameter	Value
k_R	$1.6502 \text{ M}^{-1} \text{ ms}^{-1}$
l_R	$0.10367 \times 10^{-2} \text{ ms}^{-1}$
k_A	$4185.4 \text{ M}^{-1} \text{ ms}^{-1}$
l_A	0.09512 ms^{-1}
k_I	$3.8661 \text{ M}^{-1} \text{ ms}^{-1}$
l_I	$0.4154 \times 10^{-4} \text{ ms}^{-1}$
f	0.2899
g	1.9981
h	1.1292

REFERENCES

- Balser, J. R., H. B. Nuss, D. W. Orias, D. C. Johns, E. Marban, G. F. Tomaselli, and J. H. Lawrence. 1996. Local anesthetics as effectors of allosteric gating: lidocaine effects on inactivation-deficient rat skeletal muscle sodium channels. *J. Clin. Invest.* 98:2874-2886.
- Bean, B. P., C. J. Cohen, and R. W. Tsien. 1983. Lidocaine block of cardiac sodium channels. *J. Gen. Physiol.* 81:613-642.
- Bennett, P. B., C. Valenzuela, L. Chen, and R. G. Kellen. 1995. On the molecular nature of the lidocaine receptor of cardiac sodium channels: modification of block by alterations in the alpha-subunit III-IV interdomain. *Circ. Res.* 77:584-592.
- Boland, L. M., and B. P. Bean. 1993. Modulation of N-type calcium channels in bullfrog sympathetic neurons by luteinizing hormone-releasing hormone: Kinetics and voltage dependence. *J. Neurosci.* 13:516-533.
- Cha, A., and F. Bezanilla. 1998. Structural implications of fluorescence quenching in the *Shaker* K⁺ channel. *J. Gen. Physiol.* 112:391-408.
- Clay, J. R., and L. J. DeFelice. 1983. Relationship between membrane excitability and single channel open-close kinetics. *Biophys. J.* 42:151-157.
- Corana, A., M. Marchesi, C. Martini, and S. Ridella. 1987. Minimizing multimodal functions of continuous variables with the simulated annealing algorithm. *ACM Transactions on Mathematical Software.* 13:262-280.
- Furukawa, T., S. Koumi, Y. Sakakibara, D. H. Singer, H. Jia, C. E. Arentzen, C. L. Backer, and J. A. Wasserstrom. 1995. An analysis of lidocaine block of sodium current in isolated human atrial and ventricular myocytes. *J. Mol. Cell Cardiol.* 27:831-846.

- Hanck, D. A., J. C. Makielski, and M. F. Sheets. 1994. Kinetic effects of quaternary lidocaine block of cardiac sodium channels: A gating current study. *J. Gen. Physiol.* 103:19-43.
- Hanck, D. A., M. F. Sheets, and J. C. Makielski. 1992. Phasic and tonic block of cardiac sodium channels by lidocaine correlate with immobilization of gating charge. *Circ.* 86:I-8.
- Hess, P., J. B. Lansman, and R. W. Tsien. 1984. Different modes of Ca^{+2} channel gating behavior favored by dihydropyridine Ca^{+2} agonists and antagonists. *Nature.* 311:538-544.
- Hille, B. 1977. Local anesthetics: hydrophilic and hydrophobic pathways for the drug-receptor reaction. *J. Gen. Physiol.* 69:497-515.
- Hille, B. 1992. *Ionic Channels of Excitable Membranes.* Sinauer, Sunderland, MA.
- Hondeghem, L. M., and B. G. Katzung. 1977. Time- and voltage-dependent interactions of antiarrhythmic drugs with cardiac sodium channels. *Biochim. Biophys. Acta.* 472:373-398.
- Imredy, J. P., and D. T. Yue. 1994. Mechanism of calcium-sensitive inactivation of L-type calcium channels. *Neuron.* 12:1301-1318.
- Irvine, L. A., M. S. Jafri, and R. L. Winslow. 1999. Cardiac sodium channel Markov model with temperature dependence and recovery from inactivation. *Biophys. J.* (accepted with revisions).
- Jia, H., T. Furukawa, D. H. Singer, Y. Sakakibara, S. Eager, C. Backer, C. Arentzen, and J. A. Wasserstrom. 1993. Characteristics of lidocaine block of sodium channels in single human atrial cells. *J. Pharmacol. Exp. Ther.* 264:1275-1284.

Josephson, I. R., and Y. Cui. 1994. Voltage- and concentration-dependent effects of lidocaine on cardiac Na⁺ channel and Ca⁺² channel gating charge movements. *Pflugers Arch.* 428:485-491.

Kodama, I., H. Honjo, K. Kamiya, and J. Toyama. 1990. Two types of sodium channel block by class-I antiarrhythmic drugs studied by using V_{max} of action potential in single ventricular myocytes. *J. Mol. Cell. Cardiol.* 22:1-12.

Loots, E., and E. Y. Isacoff. 1998. Protein rearrangements underlying slow inactivation of the *Shaker* K⁺ channel. *J. Gen. Physiol.* 112:377-389.

Nilius, B. 1988. Modal gating behavior of cardiac sodium channels in cell-free membrane patches. *Biophys. J.* 53:857-862.

Nilius, B., K. Benndorf, and F. Markwardt. 1987. Effects of lidocaine on single cardiac sodium channels. *J. Mol. Cell. Cardiol.* 19:865-874.

Nuss, H. B., G. F. Tomaselli, and E. Marban. 1995. Cardiac sodium channels (hH1) are intrinsically more sensitive to block by lidocaine than are skeletal muscle (?1) channels. *J. Gen. Physiol.* 106:1193-1209.

Ragsdale, D. S., J. C. McPhee, T. Scheuer, and W. A. Catterall. 1994. Molecular determinants of state-dependent block of Na⁺ channels by local anesthetics. *Science.* 265:1724-1728.

Ragsdale, D. S., J. C. McPhee, T. Scheuer, and W. A. Catterall. 1996. Common molecular determinants of local anesthetic, antiarrhythmic, and anticonvulsant block of voltage-gated Na⁺ channels. *Proc. Natl. Acad. Sci. USA.* 93:9270-9275.

Starmer, C. F., A. O. Grant, and H. C. Strauss. 1984. Mechanisms of use-dependent block of sodium channels in excitable membranes by local anesthetics. *Biophys. J.* 46:15-27.

TABLE LEGEND

Table 1: Parameters of the model of lidocaine's action.

FIGURE LEGENDS

Figure 1: State diagram for the model of lidocaine's action. *A.* The normal mode of channel gating occupied by non-drug bound channels. C_0 to C_4 are the closed states, O_1 and O_2 are the open states, C_0I to C_4I are the closed-inactivated states, and I is the inactivated state. Rate constants are as published previously (Irvine, et al., 1999). *B.* The drug mode of channel gating occupied by drug bound channels. D_1 and D_2 are the drug bound "open" states, C_0ID to C_4ID are the drug bound closed-inactivated states, and ID is the drug bound inactivated state. Rate constants are modified from those in the normal mode to preserve microscopic reversibility. *C.* Transitions between the normal and drug modes of gating. A channel can enter and exit the drug mode from the open states, the closed-inactivated states, and the inactivated state only. Each of these states has unique rates of drug binding and unbinding in accordance with the modulated receptor hypothesis (Hille, 1977; Hondeghem and Katzung, 1977). k and l are the rates of drug binding and unbinding, respectively, and g and h are scaling factors.

Figure 2: Comparison of the experimental data (O) and the model responses (\sphericalangle) for three data sets used to determine the model's parameters. *A.* Use-dependence. Each curve is fit using a single exponential. The time constants are 2.5 and 3 pulses for the experimental data and the model, respectively. *B.* Recovery from block. Each curve is fit using a single exponential. The time constants are 793 ms and 794 ms for the

experimental data and the model, respectively. C. Dose-response. The dose-response curves are fit using Eq. 6. The IC_{50} values are 166 μ M and 193 μ M for the experimental data and the model, respectively.

Figure 3: Comparison of the experimental data (O) and the model responses (\otimes) for the rate of block development due to a conditioning pulse of varying duration. A. -20 mV conditioning pulse. The curves are fit using two exponentials. The time constants of the experimental data are 5.7 ms and 181 ms. The time constants of the model are 6.2 ms and 964 ms. B. -80 mV conditioning pulse. The curves are fit using a single exponential. The time constants of the experimental data and the model are 360 ms and 357 ms, respectively.

Figure 4: Simulated steady-state availability curves in the absence of drug (O) and in the presence of 200 μ M (A) (\otimes) and 25 μ M (B) (\otimes) lidocaine. The curves are fit using a Boltzmann function. In the absence of drug, the slope factor and half-maximal potential values are 12.5 mV and 104 mV. For 200 μ M lidocaine, the slope factor and half-maximal potential values are 13 mV and 120 mV. For 25 μ M lidocaine, the slope factor and half-maximal potential values are 13.1 mV and 111.5 mV.

Figure 5: The rate of development of use-dependent block for different interstimulus intervals (ISI) and pulse durations of 3 ms (A) and 10 ms (B) simulated with the model. Pulses are from 140 mV to 20 mV. As the ISI is decreased, it takes more pulses to

reach steady-state and more block is produced. For any ISI, a longer pulse duration results in more block.

Figure 6: *A.* Comparison of simulated sodium current tracings at -30 mV in the absence of lidocaine (---) and in the presence of $25 \mu\text{M}$ (- -) and $200 \mu\text{M}$ (??) lidocaine. *B.* Normalized current-voltage curves in the absence of lidocaine (O) and in the presence of $25 \mu\text{M}$ (??) and $200 \mu\text{M}$ (??) lidocaine simulated with the model. Curves are the best fits to a modified Boltzmann function. The conductance, slope factor, and half-maximal potential are 0.0154 mV^{-1} , 7.0 mV, and -47.1 mV, respectively, in the absence of drug. For $25 \mu\text{M}$ lidocaine, the conductance, slope factor, and half-maximal potential are 0.0147 mV^{-1} , 7.1 mV, and -46.6 mV and for $200 \mu\text{M}$ lidocaine, the respective values are 0.0109 mV^{-1} , 7.6 mV, and -44.2 mV.

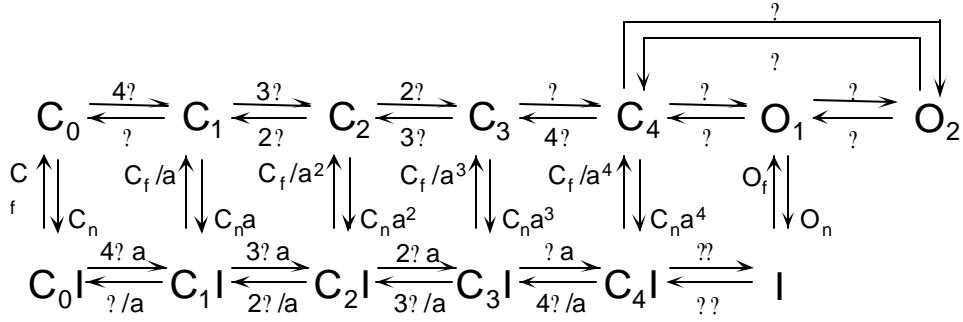
Figure 7: Simulated charge-voltage curves in the absence of lidocaine (O) and in the presence of $200 \mu\text{M}$ (A) (??) and $25 \mu\text{M}$ (B) (??) lidocaine. The curves are fit using a Boltzmann function. In the absence of drug, the maximum charge, slope factor, and half-maximal potential values are 1, 19 mV, and -75 mV. For $200 \mu\text{M}$ lidocaine, the maximum charge, slope factor, and half-maximal potential values are 0.587 , 22.3 mV and -92.1 mV. For $25 \mu\text{M}$ lidocaine, the maximum charge, slope factor, and half-maximal potential values are 0.84 , 21.8 mV and -78.5 mV.

Figure 8: Simulated single channel open duration densities at -50 mV in the absence of drug (A) and in the presence of $200 \mu\text{M}$ lidocaine (B). Twelve hundred channels are

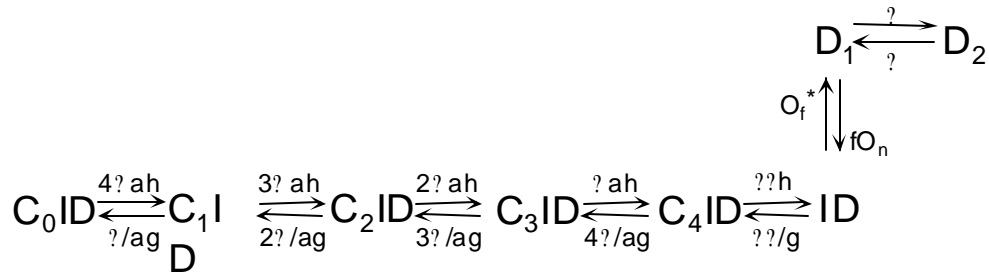
simulated for 40 ms as described in the text. Bin size is 0.5 ms. The histograms are fit using a single exponential. The time constants are 0.615 ms and 0.421 ms for no drug and 200 μ M lidocaine, respectively.

Figure 1

A Transitions within the normal mode



B Transitions within the drug mode



C All possible transitions

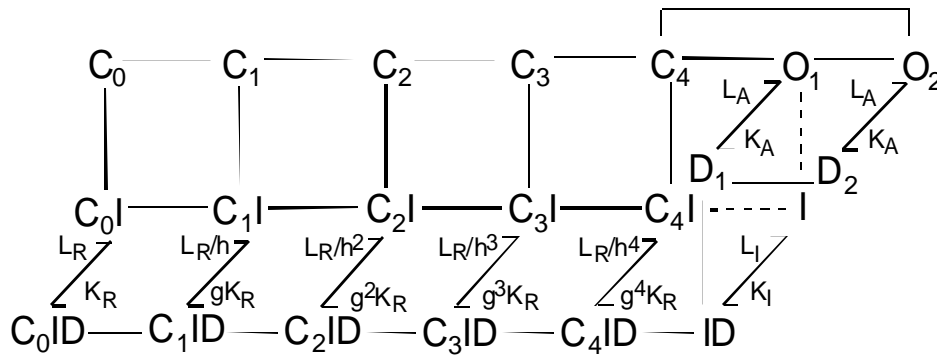


Figure 2

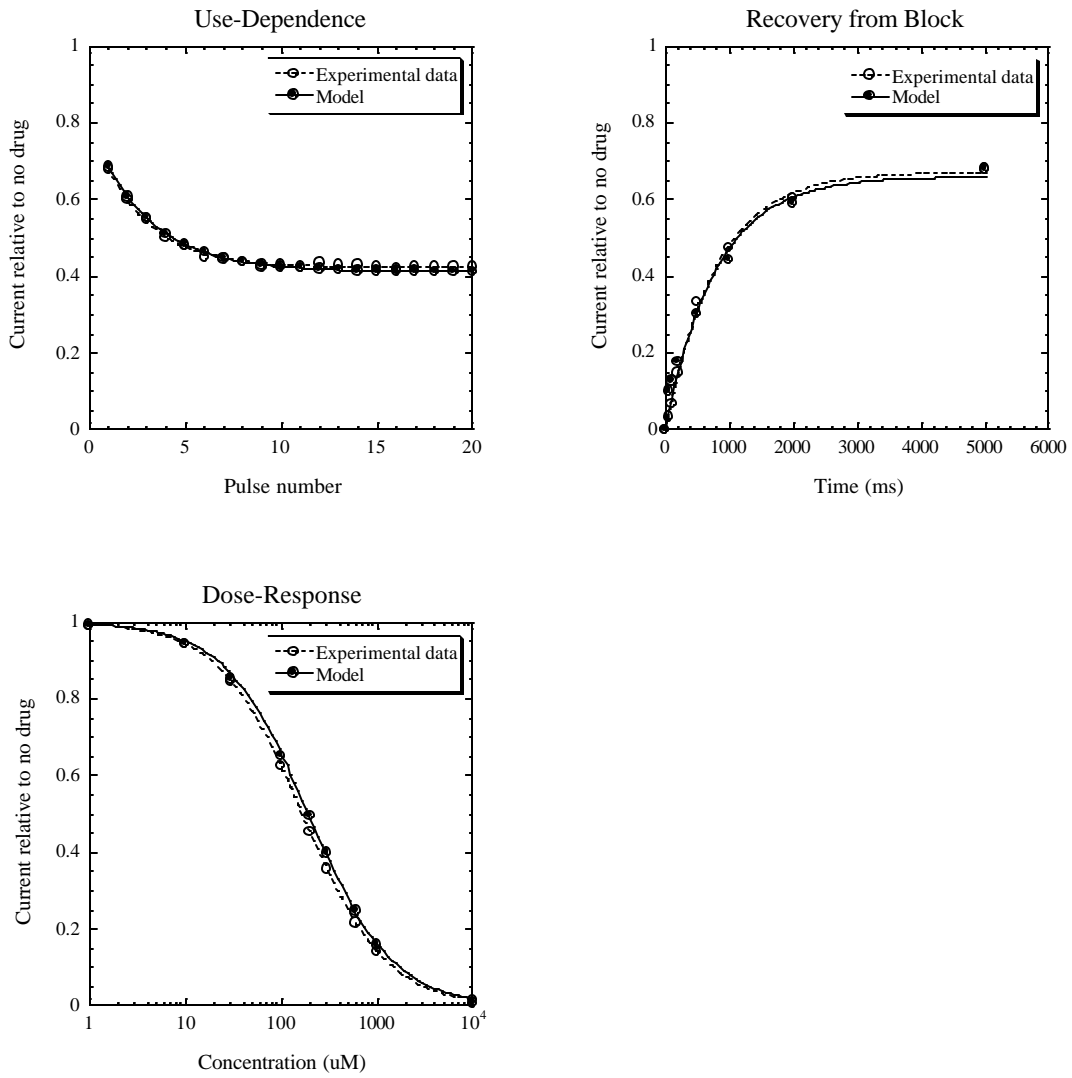


Figure 3

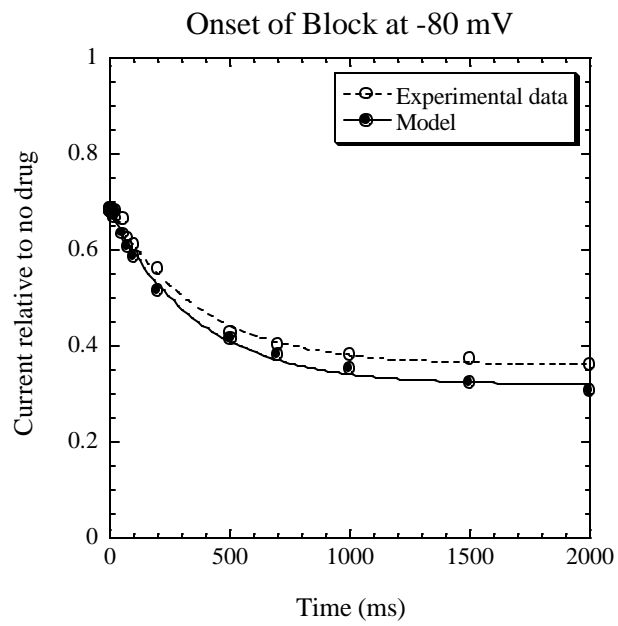
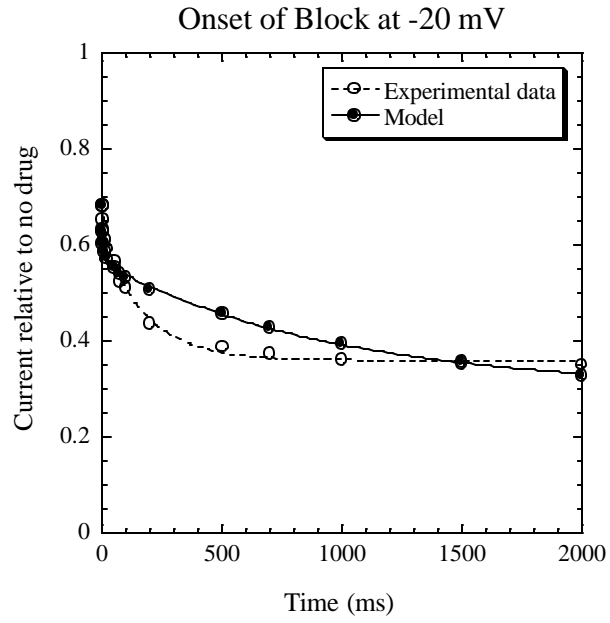


Figure 4

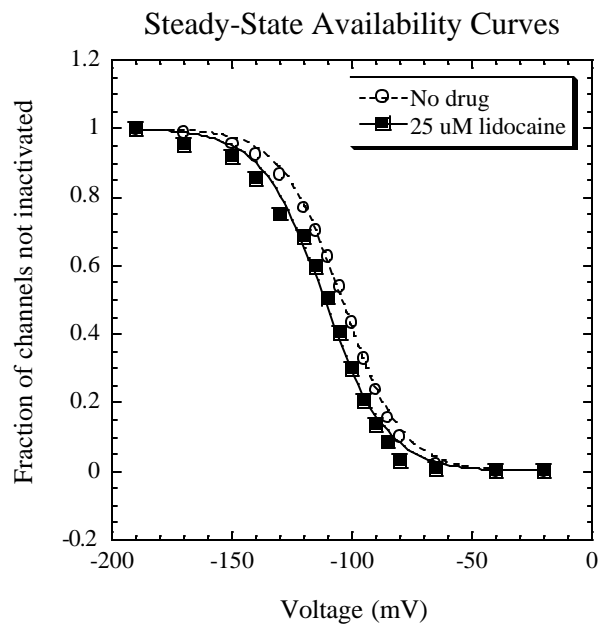
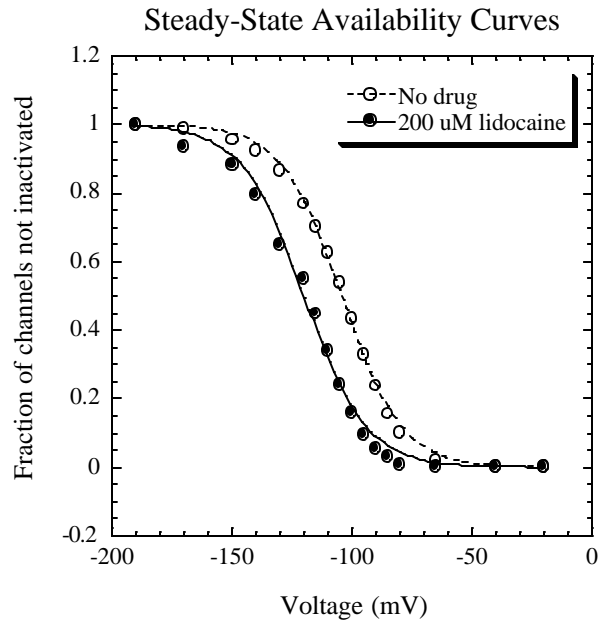


Figure 5

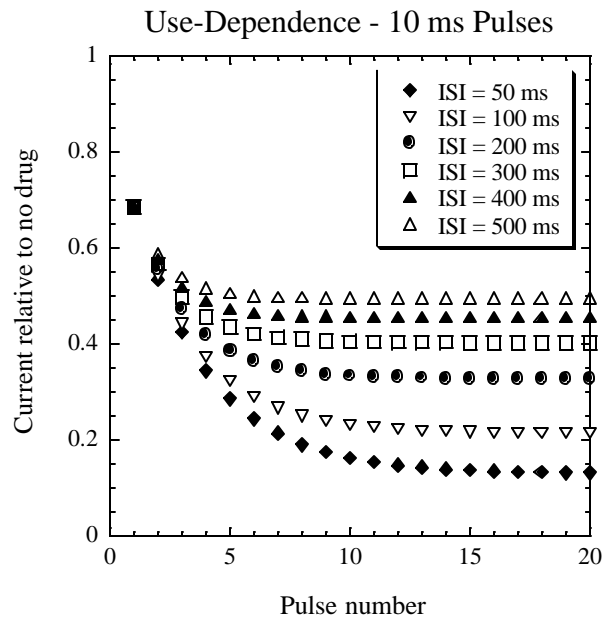
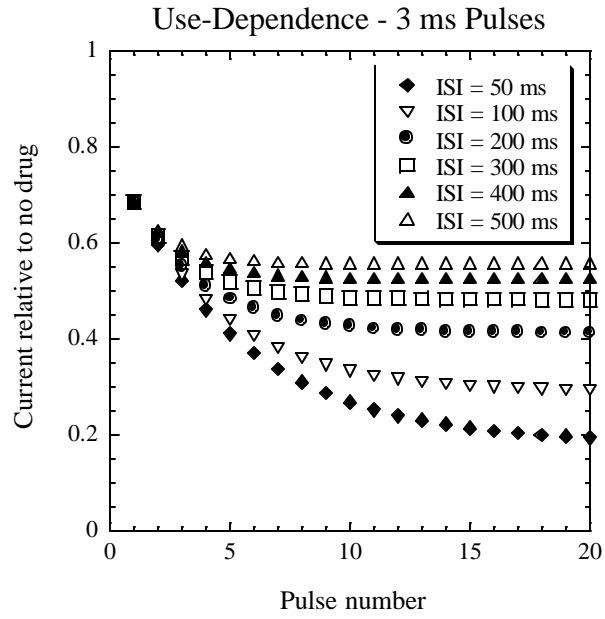


Figure 6

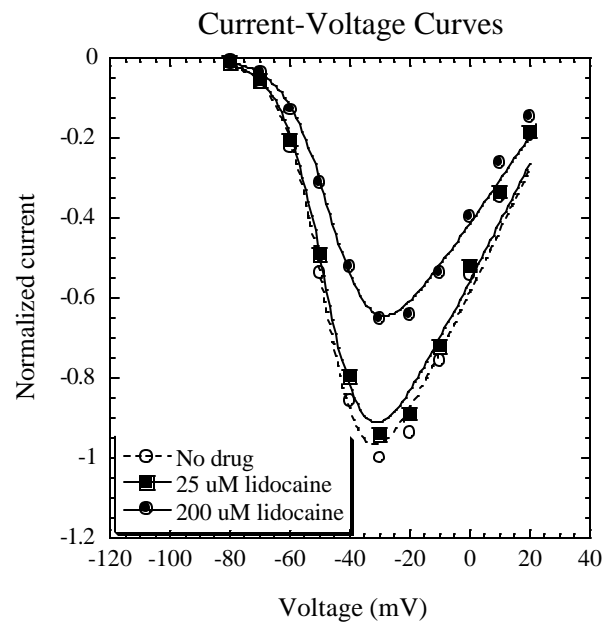
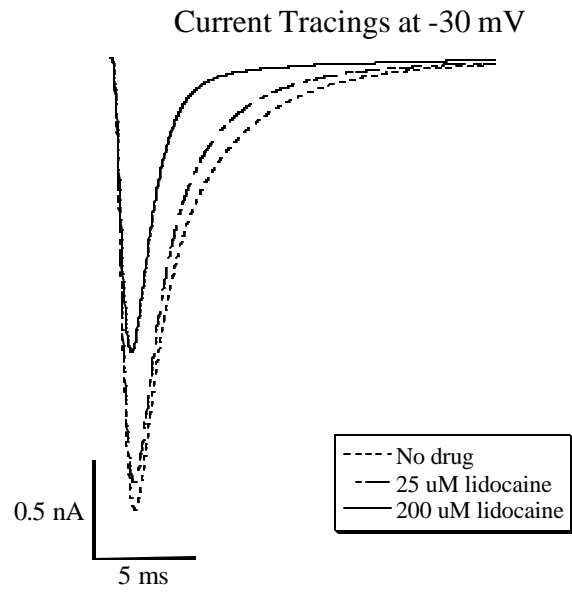


Figure 7

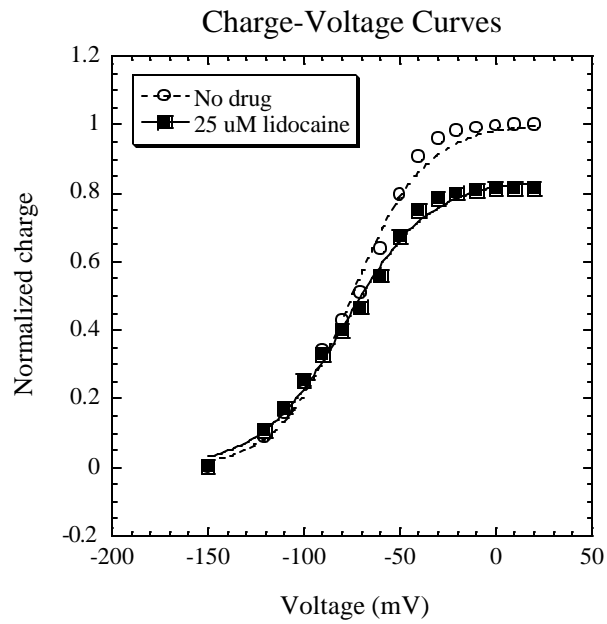
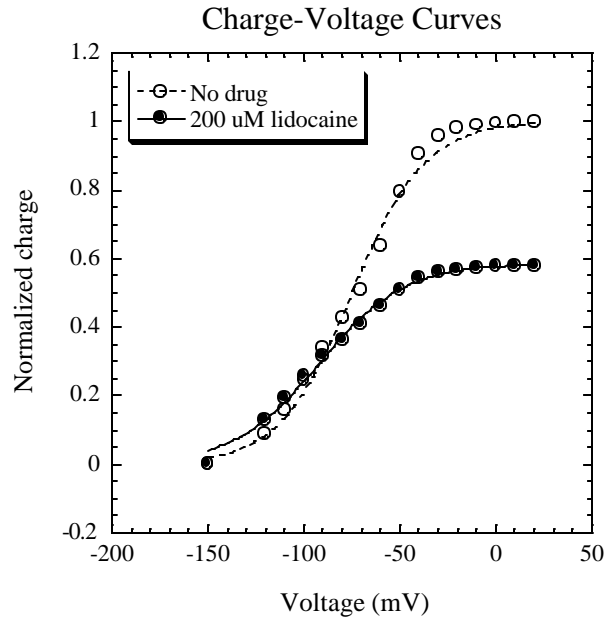


Figure 8

